Journal of Experimental Botany, Vol. 69, No. 8 pp. 2071–2083, 2018
doi:10.1093/jxb/ery039 Advance Access publication 6 March 2018
This paper is available online free of all access charges (see http://jxb.oxfordjournals.org/open_access.html for further details)

RESEARCH PAPER

Hypoxia in grape berries: the role of seed respiration and lenticels on the berry pedicel and the possible link to cell death

Zeyu Xiao[1,2], Suzy Y. Rogiers[1,3,4], Victor O. Sadras[1,2,5] and Stephen D. Tyerman[1,2,*]

[1] The Australian Research Council Training Centre for Innovative Wine Production, The University of Adelaide, Glen Osmond, SA, Australia
[2] School of Agriculture, Food and Wine, Waite Research Institute, The University of Adelaide, PMB1, Glen Osmond, SA 5064, Australia
[3] NSW Department of Primary Industries, Wagga Wagga, NSW, Australia
[4] National Wine and Grape Industry Centre, Charles Sturt University, Wagga Wagga, NSW 2678, Australia
[5] South Australian Research & Development Institute, Waite Research Precinct, Urrbrae, SA 5064, Australia

* Correspondence: steve.tyerman@adelaide.edu.au

Received 26 October 2017; Editorial decision 19 January 2018; Accepted 31 January 2018

Editor: Robert Hancock, The James Hutton Institute, UK

Abstract

Mesocarp cell death (CD) during ripening is common in berries of seeded *Vitis vinifera* L. wine cultivars. We examined if hypoxia within berries is linked to CD. The internal oxygen concentration ($[O_2]$) across the mesocarp was measured in berries from Chardonnay and Shiraz, both seeded, and Ruby Seedless, using an oxygen micro-sensor. Steep $[O_2]$ gradients were observed across the skin and $[O_2]$ decreased toward the middle of the mesocarp. As ripening progressed, the minimum $[O_2]$ approached zero in the seeded cultivars and correlated to the profile of CD across the mesocarp. Seed respiration declined during ripening, from a large proportion of total berry respiration early to negligible at later stages. $[O_2]$ increased towards the central axis corresponding to the presence of air spaces visualized using X-ray micro-computed tomography (CT). These air spaces connect to the pedicel where lenticels are located that are critical for berry O_2 uptake as a function of temperature, and when blocked caused hypoxia in Chardonnay berries, ethanol accumulation, and CD. The implications of hypoxia in grape berries are discussed in terms of its role in CD, ripening, and berry water relations.

Keywords: Grape berry, lenticels, micro-CT, oxygen sensor, pedicel, programmed cell death, respiration, seed respiration, temperature, *Vitis vinifera*.

Introduction

Onset and rate of cell death (CD) in berry mesocarp of *Vitis vinifera* L. are genotype dependent, and modulated by temperature and drought (Krasnow *et al.*, 2008; Tilbrook and Tyerman, 2008; Fuentes *et al.*, 2010; Bonada *et al.*, 2013*a, b*). Evolutionarily, CD may have been selected as a trait favouring seed dispersal (Hardie *et al.*, 1996). It correlates with berry dehydration (Fuentes *et al.*, 2010; Bonada *et al.*, 2013*a*), a common phenomenon in warm wine-growing regions, and is partially distinct from other forms of 'berry shrivel' (Bondada and Keller, 2012; Keller *et al.*, 2016). Berry dehydration associated with CD is common in Shiraz (Syrah), resulting in increased sugar concentration (Rogiers *et al.*, 2004; Sadras and McCarthy, 2007; Caravia *et al.*, 2016). It is also associated with altered chemical composition (Šuklje *et al.*, 2016) and sensory characteristics (Bonada *et al.*, 2013*b*).

© The Author(s) 2018. Published by Oxford University Press on behalf of the Society for Experimental Biology.
This is an Open Access article distributed under the terms of the Creative Commons Attribution License (http://creativecommons.org/licenses/by/4.0/), which permits unrestricted reuse, distribution, and reproduction in any medium, provided the original work is properly cited.

Downloaded from https://academic.oup.com/jxb/article-abstract/69/8/2071/4837303
by University of Adelaide user
on 16 August 2018

Grape berries are non-climacteric, though ethylene may still play a role (Bottcher *et al.*, 2013). However, the onset of ripening is associated with the accumulation of hydrogen peroxide (H_2O_2) in skin of Pinot Noir berries (Pilati *et al.*, 2014). Although H_2O_2 was considered a harmless signal, Pinot Noir berries also show up to 50% CD (Fuentes *et al.*, 2010). Accumulation of H_2O_2 is also characteristic of plant tissues exposed to hypoxia or anoxia (Blokhina *et al.*, 2001; Fukao and Bailey-Serres, 2004). The grape berry respiratory quotient increased during ripening (Harris *et al.*, 1971) associated with increased ethanolic fermentation (Terrier and Romieu, 2001; Famiani *et al.*, 2014). Other fruit also show restricted aerobic respiration and fermentation (Hertog *et al.*, 1998). Ethanolic fermentation contributes to maintain cell function under O_2-limiting conditions provided sugars are available. Interestingly, both H_2O_2 and ethylene have been implicated in its regulation (Fukao and Bailey-Serres, 2004).

Hypoxia-induced oxidative stress decreases lipid and membrane integrity (Blokhina *et al.*, 2001), the latter being clearly evident in most wine grape berries by vitality stains (Tilbrook and Tyerman, 2008). Increased CD in Shiraz grapes is reflected by decreased extracellular electrical resistance indicating electrolyte leakage (Caravia *et al.*, 2015). This leakage corresponds to the accumulation of potassium in the extracellular space of Merlot berries (Keller and Shrestha, 2014), a cultivar that also displayed CD (Fuentes *et al.*, 2010). O_2 deprivation diminishes intracellular energy status that reduces cell vitality in non-photosynthetic organs, as exemplified by roots under flooding or waterlogging (Voesenek *et al.*, 2006). Although grape berries show some photosynthesis in early stages of development (Ollat and Gaudillère, 1997), during ripening photosynthetic pigments and nitrogen content are reduced and atmospheric CO_2 is not fixed, while re-fixation of respiratory CO_2 declines (Palliotti and Cartechini, 2001).

Shiraz berry CD can be accelerated by water stress and elevated temperature (Bonada *et al.*, 2013*b*). There are increasing frequencies and intensities of heat waves and drought events globally including Australia (Alexander and Arblaster, 2009; Perkins *et al.*, 2012), and the warming trend is predicted to have adverse effects on grapevines (Webb *et al.*, 2007) and berry quality (Fuentes *et al.*, 2010; Bonada and Sadras, 2015; Caravia *et al.*, 2016). Higher temperature increases demand for O_2 to support increased oxidative respiration (Kriedemann, 1968). Meanwhile, O_2 diffusion into the berry may be limited by decreased gas exchange across the berry skin during ripening, as judged by declining transpiration (Rogiers *et al.*, 2004; Scharwies and Tyerman, 2017) and/or changes in berry internal porosity during ripening. Lenticels on the skin of potato tubers are the main channel for O_2 uptake for respiration (Wigginton, 1973), and the phellem–lenticel complex of woody roots and trunks regulates O_2 exchange (Lendzian, 2006). In the grape berry, the small number of stomata on skin develop into non-functional lenticels occluded with wax (Rogiers *et al.*, 2004), but lenticels are very prominent on the pedicel (Becker *et al.*, 2012).

Wine grape cultivars are seeded, and have been selected for wine-related attributes, whereas table grape cultivars have been selected for turgor maintenance, and markets increasingly demand seedless fruit; these differences in selective pressures between wine and table grape cultivars have led to differences in the dynamics of water during berry ripening (Sadras *et al.*, 2008). Table grape seedless cultivars show little or no CD well into ripening (Tilbrook and Tyerman, 2008; Fuentes *et al.*, 2010). Although lignification of seeds is complete before berries begin to ripen (Cadot *et al.*, 2006), oxidation of seed tannins is sustained (Ristic and Iland, 2005) and is concurrent with oxidation of phenolic compounds such as flavan-3-ol monomers and procyanidins (Cadot *et al.*, 2006). Lignin polymerization requires consumption of O_2 and generation of H_2O_2 for the final peroxidase reaction (Lee *et al.*, 2013), and this, with oxidation of tannins, could put additional stress on the mesocarp in seeded cultivars. Phenolic compounds can also act as reactive oxygen species (ROS) scavengers (Blokhina *et al.*, 2003). In grape, biosynthesis of procyanidins coincides with the initial rapid period of growth (Coombe, 1973), and flavan-3-ol accumulated during early ripening (Cadot *et al.*, 2006). Taken together, seed respiration and maturation deserve consideration in understanding mesocarp CD.

In this study, we test the hypothesis that hypoxia {i.e. below normoxia as 20.95% air O_2 concentration [O_2] (Sasidharan *et al.*, 2017)} occurs within the grape berry during ripening and that this may be correlated with CD in the pericarp. We compared the patterns of CD and [O_2] profiles across the berry flesh of two wine, seeded cultivars, Chardonnay and Shiraz, and a seedless table grape cultivar, Ruby Seedless. Respiratory demand of seeds and berries were measured for different ripening stages and different temperatures. The diffusion pathway of O_2 supply was assessed through examination of the role of lenticels in the berry pedicel and air space estimates using X-ray micro-computed tomography (micro-CT) of single berries.

Materials and methods

Berries from vineyards

Details of sources of berries, vine age, sampling times, and corresponding measurements are listed in Table 1. Berries from the Waite Campus (34°58'04.8"S, 138°38'07.9"E) vineyards were sampled over the 2014–2015, 2015–2016, and 2016–2017 seasons. Mature Shiraz, Chardonnay, and Ruby Seedless vines on their own roots were grown under standard vineyard management with vertical shoot positioning, spur pruning (two buds), and drip irrigation on dark brown clay soils with shale fragments, grading into red-brown mottled clay; overlying olive-brown mottled cracking clay (Du Toit, 2005). Rows (3 m spacing) were north–south oriented. Three replicates each consisted of two vines per replicate for Shiraz and three vines per replicate for Chardonnay. Ten random clusters (combination of proximal and distal) were labelled within each replicate, and 20 berries (two from each cluster, randomly located within the cluster) per replicate were excised at the pedicel–rachis junction with sharp scissors at each sampling date between 09.00 h and 11.00 h. Ruby Seedless grapes were sampled from three vines with five clusters labelled for sampling on each vine, and 20 berries were sampled from each vine. Timing of sampling during berry development was measured as days after anthesis (DAA, 50% of caps fallen from flowers). Berries were placed in sealed plastic bags into a cooled container, and taken to the laboratory, stored at 4 °C in the dark, and tested within 48 h of sampling.

Berries from pot-grown vines

Shiraz and Chardonnay cuttings were taken from the Waite vineyards in April 2015 and propagated after storage at 4 °C in the dark for ~2 weeks.

Downloaded from https://academic.oup.com/jxb/article-abstract/69/8/2071/4837303
by University of Adelaide user
on 16 August 2018

Table 1. *Summary of berry source and traits measured*

Source of berries	Cultivar	Plant date	Season	Traits	Sampling time	Replication
Waite vineyards	Chardonnay	1995	2015–2016;	O_2 profile	87, 104, 136 DAA	3 reps, 3 berries
			2016–2017	Berry and seed respiration	63, 122 DAA	per rep
				Micro-CT	98, 154 DAA	3 reps, 1 berry
				O_2 profile when N_2 applied	90 DAA	per rep
				Respiration (lenticel blockage)	86 DAA	
				Respiration (temperature change)	76, 120 DAA	
	Shiraz	1993	2014–2015;	O_2 profile	85, 114 DAA	3 reps, 3 berries
			2016–2017	Respiration (lenticel blocked)	77 DAA	per rep
				Respiration (temperature change)	71, 113 DAA	
	Ruby seedless	1992	2016–2017	O_2 profile	91, 132 DAA	3 reps, 3 berries
				O_2 logging	132 DAA	per rep
Growth chamber, cuttings from Waite vineyard	Chardonnay	2015	2015	Lenticel	At veraison	5 berries
	Shiraz	2015	2015	Lenticel	At veraison	5 berries
Growth chamber, rootlings from Yalumba	Chardonnay	2017	2017	Lenticel blockage on vines (O_2, cell vitality, ethanol)	3, 5, 7, 10, 12, 14, 18, and 20 d after blockage	2 or 3 berries

The propagation method and vine nutrition management were based on Baby *et al.* (2014). Briefly, after roots were initiated in a heated sand bed in a 4 °C cold room for 8 weeks, and after the root length reached ~6 cm, cuttings were transferred into a vermiculite:perlite (1:1) mixture in 12 cm pots. Pots were placed in a growth chamber with a 16 h photoperiod, 400 µmol photons m^{-2} s^{-1}) at the plant level, 27 °C day/22 °C night, and 50% humidity. Pots were irrigated with half-strength Hoagland solution (Baby *et al.*, 2014). Fruitful vines at stage EL-12 (Coombe, 1995) were then transferred into a University of California (UC) soil mix: 61.5 litres of sand, 38.5 litres of peat moss, 50 g of calcium hydroxide, 90 g of calcium carbonate, and 100 g of Nitrophoska® (12:5:1, N:P:K plus trace elements; Incitec Pivot Fertilisers, Southbank, Vic., Australia), per 100 litres at pH 6.8, in 20 cm diameter (4 litre) pots irrigated with water thereafter. Five berries (each from three different vines) of each cultivar were used for light stereomicroscopy.

Chardonnay rootlings were obtained from Yalumba Nursery in April 2017 and planted with UC mix soil and in the same growth chamber with the same growth conditions as above. Seven vines, each with one cluster, were used for O_2 diffusion experiments.

$[O_2]$ profiles in berries

Berry $[O_2]$ was measured using a Clark-type O_2 microelectrode with a tip diameter of 25 µm (OX-25; Unisense A/S, Aarhus, Denmark). The microelectrodes were calibrated in a zero O_2 solution (0.1 M NaOH, 0.1 M $C_6H_7NaO_6$) and an aerated Milli-Q water (272 µmol l^{-1} at 22 °C), as 100% O_2 solution. Individual berries (equilibrated to room temperature) were secured on the motorized micromanipulator stage. To aid the penetration of the microelectrode into the berry skin, the skin was pierced gently with a stainless-steel syringe needle (19 G), to a depth of 0.2 mm, at the equator of the berry. The microsensor was positioned in the berry through this opening and $[O_2]$ profiles were taken with depth towards the centre of the berry. For Shiraz, measurements were taken from 0.2 mm to 1.5 mm under the skin at 0.1 mm increments. The electrode was not moved beyond this point to avoid damaging the tip against a seed. For Ruby Seedless, where seeds were not present, and Chardonnay grapes, where there were no seeds present or the position of the seeds could be determined through the semi-transparent skin, measurements were taken at 0.5 mm intervals from 0.2 mm under the skin to the berry centre. Each measurement was applied for a 10 s duration at each depth. Between each position, a 20 s waiting time was applied to ensure stable signals. To test whether puncturing of the skin by the needle and insertion of the microelectrode contaminated the berry internal O_2 by the surrounding air, a plastic ring was placed around the insertion site and a gentle stream (250 ml min^{-1}) of nitrogen gas was applied to the insertion point while obtaining the O_2 readings (Fig. 1A). These readings were compared with those where no nitrogen gas was applied.

The O_2 readings were recorded using the Unisense Suite software (Unisense A/S). Three berries were measured for each biological replicate.

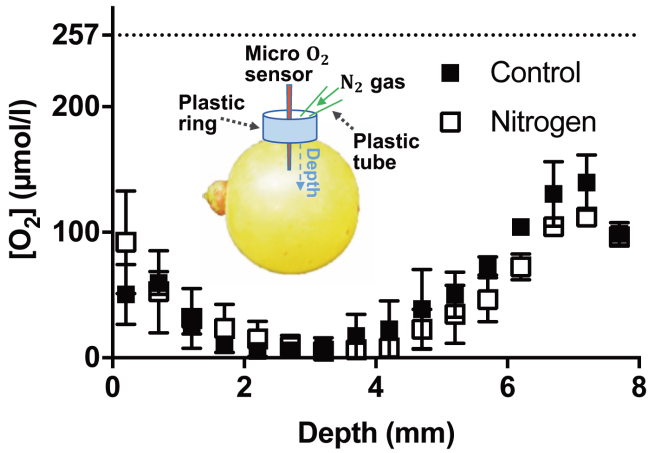

Fig. 1. $[O_2]$ profiles of Chardonnay berries (90 DAA in the 2016–2017 season, Waite vineyards) measured with and without N_2 gas applied at the entry point during measurement. Inset: experimental set-up for measuring berry $[O_2]$ profiles (not to scale). The O_2 sensor (tip diameter 25 µm) was inserted at the equator of the berry and moved inwards to the centre approximately across the radius. Around the entry of the sensor, a plastic ring was sealed and glued to the berry, to contain nitrogen gas gently flowing on to the entry point of the sensor. Data are means ±SE, n=3. Two-way ANOVA (repeated measures) showed that depth accounted for 68.73% of total variation (P<0.0001), treatments accounted for 0.55% of total variation (P=0.26), and interaction accounted for 3.72% of total variation (P=0.87). (This figure is available in colour at *JXB* online.)

Means and SE of each step (n=3) were calculated and $[O_2]$ profiles were compiled using GraphPad Prism 7 (GraphPad Software Inc., La Jolla, CA, USA). Following the O_2 measurements, berry temperature was recorded using an IR thermometer (Fluke 568, Fluke Australia Pty Ltd, NSW, Australia) with a type-K thermocouple bead probe (Fluke 80PK-1). Berry diameters at the equator were measured with a digital calliper. $[O_2]$ and respiration (see below) were measured under dim room lighting, <1 µmol photon m^{-2} s^{-1}. Berry vitality was determined (see below) and total soluble solids (TSS) of the juice from individual berries were determined using a digital refractometer (Atago, Tokyo, Japan) as an indicator of berry maturity.

Testing the role of pedicel lenticels

$[O_2]$ was measured as above but with the probe stationary at ~2 mm from the pedicel along the berry central axis. After a stable reading was obtained, N_2 gas (250 ml min^{-1}) was then applied over the pedicel

Downloaded from https://academic.oup.com/jxb/article-abstract/69/8/2071/4837303
by University of Adelaide user
on 16 August 2018

in order to test the contribution of pedicel lenticels to O_2 diffusion into the berry.

Berry and seed respiratory O_2 consumption

A Clark-type oxygen microsensor OX-MR and the MicroRespiration System (Unisense A/S) were used for berry and seed respiration measurements. A replicate consisted of nine berries. The measuring chamber was filled with aerated MilliQ water, constantly stirred, and was maintained at 25 °C in a water bath. After the measurement of whole berry respiration, seeds of the nine berries were extracted and the seed respiration rate measured using the same apparatus. Changes in the chamber's water $[O_2]$ were monitored for at least 15 min, with readings taken every 5 s in order to determine a steady respiration rate from the slope of the decline in $[O_2]$.

Respiration was also measured for Shiraz and Chardonnay berries before and after the pedicels were covered with silicone grease (SGM494 silicone grease, ACC Silicones Limited, Bridgewater, UK), which was known to restrict berry pedicel water uptake (Becker *et al.*, 2012), at 20 °C and 40 °C. Another batch of nine Chardonnay berries was used to determine the respiratory contribution of excised pedicels.

The temperature dependence of berry respiration was determined with a water bath held at 10, 20, 30, and 40 °C.

Pedicel lenticel density

The lenticel density of Chardonnay and Shiraz berry pedicels (stem and receptacle) was assessed using a Nikon SMZ 25 stereo microscope with CCD camera (Nikon Instruments Inc., Melville, NY, USA). Lenticel area (%) was estimated using ImageJ (Schneider *et al.*, 2012) by first adjusting the colour threshold of the image to separate the pedicel from the background and then the lenticels from the pedicel. Subsequently the region of interest (ROI) managing tool was used to estimate the relative area of the pedicels and the lenticels.

Long-term effect of blocking pedicel lenticels

The pedicel of approximately half of the berries on each cluster of growth chamber-grown Chardonnay were covered with silicone grease at the onset of ripening (first signs of berry softening). Two or three pairs of berries, each pair containing one covered and one uncovered (control) pedicel from one plant, were randomly sampled throughout the course of the experiment at 3, 5, 7, 10, 12, 14, and 18 d after application. Profiles of berry $[O_2]$ were measured as above, and berries were subsequently assessed for cell vitality (see below). Three pairs of berries were sampled 12 d and 20 d after silicone application and assessed for internal ethanol concentration (see below).

Berry ethanol concentration

Individual berries were ground to a fine powder under liquid nitrogen. Ethanol was quantified using an Ethanol Assay kit following the manufacturer's instructions (Megazyme International Ireland Ltd, Wicklow, Ireland). Briefly, alcohol dehydrogenase (ADH) catalysed the oxidation of ethanol to acetaldehyde. Acetaldehyde was then further oxidized to acetic acid and NADH in the presence of aldehyde dehydrogenase (AL-DH) and NAD^+. NADH formation was measured in a FLUOstar Omega plate reader (BMG LABTECH GmbH, Ortenbery, Germany) at 340 nm.

Pericarp cell vitality estimation

Cell vitality was estimated using a fluorescein diacetate (FDA) staining procedure on the cut medial longitudinal surface of berries as detailed in Tilbrook and Tyerman (2008) and Fuentes *et al.* (2010). Images were analysed with a MATLAB (Mathworks Inc., Natick, MA, USA) code for determining berry cell vitality (Fuentes *et al.*, 2010). Using ImageJ, the FDA fluorescence signal across the radius at the equator was analysed. The correlation between $[O_2]$ and fluorescence signal at corresponding distances within Chardonnay and Ruby Seedless berries were examined. The fluorescence signal of growth chamber-grown Chardonnay berries with or without the pedicel covered was also analysed in this way.

Air spaces within the berry

Chardonnay berries were sampled during the 2015–2016 season for micro-CT, where three berries, each from a different replicate, were used for each sampling time. Grapes were imaged with a Skyscan 1076 (Bruker micro-CT, Kontich, Belgium) at the micro-CT facility at Adelaide Microscopy, where whole berries (pedicel attached) had 2-D projections acquired with 59 kV, 149 μA, Al 0.5 mm filter, 2356 ms exposure, 0.4° rotation step, and 8.5 μm pixel size (equivalent to 15 μm spatial resolution or 3×10^{-6} mm^3 voxel size). NRecon (bruker-microct.com) was used for greyscale image reconstruction. Using CT-Analyer (bruker-microct.com), Otsu thresholding was applied to the volume and despeckle was applied to accept only continuous volume over 500 voxels as connected air spaces. Three-dimensional images of the internal air spaces were generated using CTVox (bruker-microct.com); colour rendering modules were used to distinguish the internal air volume from the berry volume. The 3-D models were then longitudinally sectioned to reveal the internal air space distribution. Quantitative analysis of internal porosity between the berry proximal region and the top (hilum) of the seed(s) was performed by manually selecting the volume of interest and accepting 500 voxels as air spaces.

Statistical analysis

All data are presented as the mean ±SE. Two-way ANOVA was used for: effect of O_2 sensor depth and applying N_2 gas at the point of sensor entry on $[O_2]$, effect of O_2 sensor depth and ripening stage on $[O_2]$, effect of temperature and covering lenticels on respiration, effect of temperature and grape maturity on respiratory Q_{10}, effect of covering lenticels and the duration of coverage on $[O_2]$, TSS, sugar per berry, ethanol, and living tissue profiles. Deming regression was used to determine the association between fluorescent intensity of FDA stain and $[O_2]$; this type of regression takes account of error in both x and y (Strike, 1991). t-test was used for differences in: respiration of berry and seed of Chardonnay at two ripening stages, lenticel area on pedicels between Chardonnay and Shiraz, activation energy of O_2 uptake of Chardonnay and Shiraz berries, and porosity and connectivity index in Chardonnay at two ripening stages. Rates of CD in lenticel-covered berries and control berries were determined using linear regression.

Results

Internal oxygen profiles of grape berries

In Chardonnay, $[O_2]$ decreased from the skin towards the interior of the mesocarp to reach a low concentration at depths of 2.2–4 mm (Fig. 1). The minimum $[O_2]$ over this depth range was 5.5 ± 5.5 μmol l^{-1}. However, with further penetration towards the central axis of the berry, $[O_2]$ increased and reached a maximum at 7 mm depth (Fig. 1). To test if the $[O_2]$ profiles were affected by introduced O_2 via the penetration site, N_2 gas was gently applied on to the entry point of the sensor during the measurements. The $[O_2]$ profiles were similar for control and nitrogen-treated berries (Fig. 1), indicating that leakage through the site of penetration did not affect the recorded profiles.

Changes in internal oxygen profiles and progression of cell death during ripening

To uncover whether there was a link between the progression of CD and hypoxia within the berry, we determined CD

Downloaded from https://academic.oup.com/jxb/article-abstract/69/8/2071/4837303
by University of Adelaide user
on 16 August 2018

using FDA staining and recorded [O_2] profiles on berries sampled on the same days. Similar [O_2] profiles were observed for Chardonnay and Ruby Seedless (Fig. 2A, C), and for Shiraz over the first 1.5 mm (Fig. 2E), but the [O_2] dropped more steeply across the skins as ripening progressed in all cultivars, resulting in overall lower [O_2] across the berry. This was manifest as a much lower minimum [O_2] at the last ripening stage sampled: Chardonnay 0 μmol l^{-1}, Ruby Seedless 14.9 ± 8.86 μmol l^{-1}, and Shiraz 0 μ μmol l^{-1}. Because seeds could not be visualized in Shiraz berries, the micro oxygen sensor could not be moved further into the berry than ~1.6 mm without risking the integrity of the sensor (Fig. 2E). Nevertheless, it was clear that [O_2] dropped precipitously towards 1 mm (Fig. 2E).

Vitality staining (Fig. 2B, F) indicated that, for both Chardonnay and Shiraz, CD increased over time as TSS accumulated, and occurred predominantly in the middle of the mesocarp corresponding to the minimum in [O_2]. Further, the change in fluorescent signal intensity across the radius at the equator of Chardonnay berries showed a similar trend as for berry internal [O_2] (Fig. 3A), indicating a correlation between cell vitality and internal [O_2] (Fig. 3B). On the other hand, Ruby Seedless berries maintained cell vitality close to 100% up to 132 DAA, when TSS was 20.7 °Brix (Fig. 2D). While a similar shape of [O_2] profile was observed within the mesocarp of Ruby Seedless berries when compared with that of Chardonnay berries (Fig. 2C), [O_2] did not reach zero.

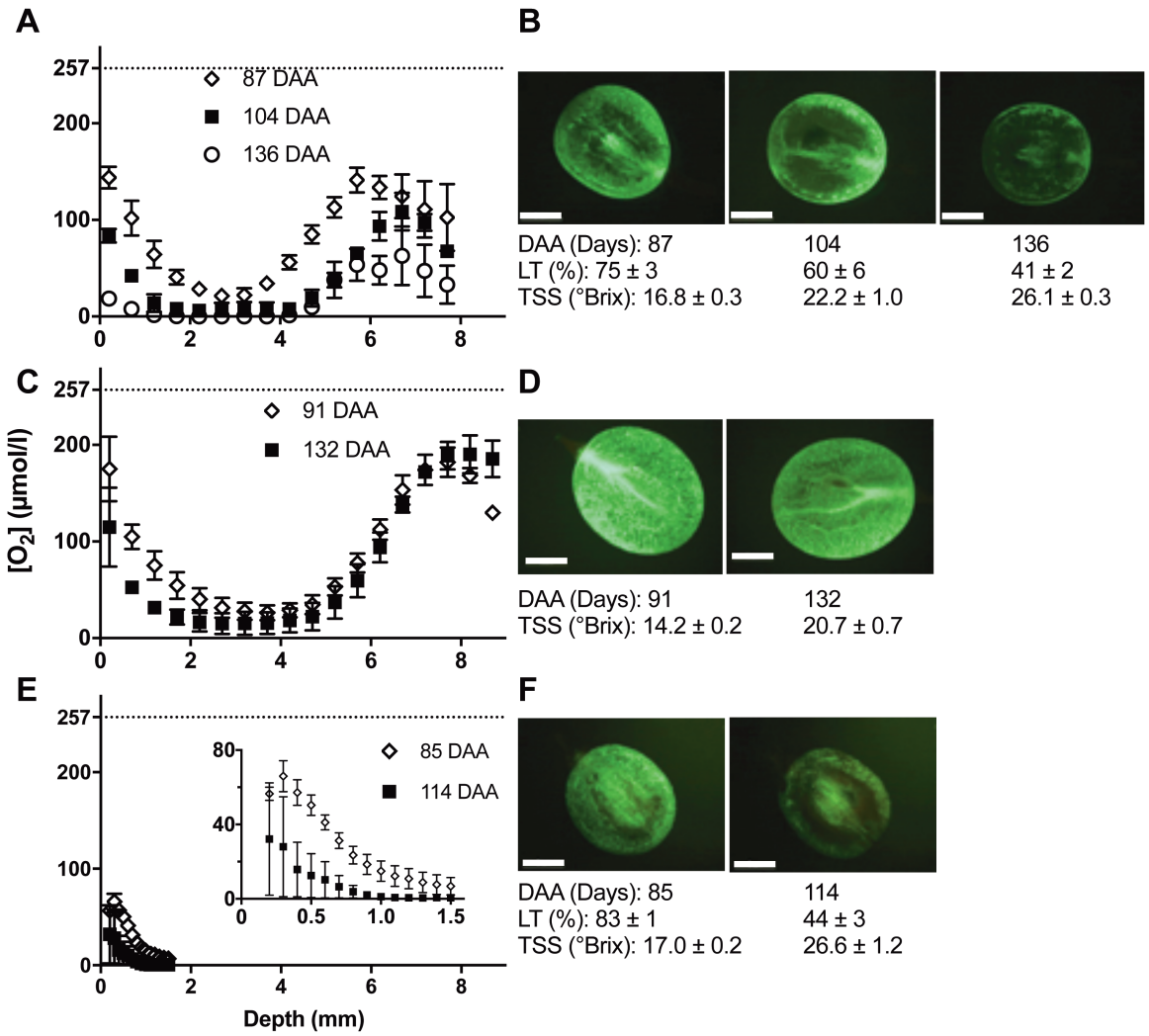

Fig. 2. [O_2] profiles of Chardonnay, Ruby Seedless, and Shiraz berries (A, C, E) at various ripening stages and corresponding examples of living tissue (LT) in the pericarp for each variety (B, D, F). (A) Chardonnay berries were sampled at 87, 104, and 136 DAA in the 2015–2016 season. Two-way ANOVA (repeated) showed that depth accounted for 46.7% of total variation (P<0.0001), time accounted for 29.9% of total variation (P<0.0001), and interaction accounted for 8.0% of total variation (P=0.058). The horizontal dashed line indicates the approximate O_2 saturation value for Millipore water at room temperature, the same as berries at the time of measurement. (B) Medial longitudinal sections (Chardonnay) stained with FDA, highlighting LT differences at different stages of ripening (corresponding to A). (C) [O_2] profiles of Ruby Seedless berries sampled at 91 and 132 DAA in the 2016–2017 season. Two-way ANOVA (repeated) showed that depth accounted for 85.2% of total variation (P<0.0001), time accounted for 1.2% of total variation (P=0.0025), and interaction accounted for 3.7% of total variation (P=0.048). (D) LT of Ruby Seedless was close to 100% for the two respective sampling days. (E) [O_2] profiles of Shiraz berries sampled on 85 and 114 DAA in the 2014–2015 season. Inset shows detail of the profile to 1.5 mm. Two-way ANOVA (repeated) showed that depth accounted for 40.9% of total variation (P=0.0005), time accounted for 19.6% of total variation (P<0.0001), and interaction accounted for 6.4% of total variation (P=0.43). (F) LT of Shiraz. Data are means ±SE, n=3 for (A), (C), and (E).

Downloaded from https://academic.oup.com/jxb/article-abstract/69/8/2071/4837303
by University of Adelaide user
on 16 August 2018

Despite the decrease in [O_2] across the mesocarp during ripening, for Chardonnay and Ruby Seedless berries, [O_2] started to increase with depth from ~4.2 mm and reached a maximum at ~6.2 mm in Chardonnay and 8.2 mm in the larger Ruby Seedless berries (Fig. 2A, C). Standardizing the position of the sensor relative to the diameter of each berry replicate (Fig. 4) showed that [O_2] peaked at the central vascular bundle region at all sampling times for both Chardonnay (Fig. 4A) and Ruby Seedless (Fig. 4B).

Consumption and supply pathways of oxygen within grape berries

Considering the link between CD and [O_2] (Fig. 3), and the lack of CD in well-developed berries of Ruby Seedless (Fig. 2D), we investigated the contribution of seeds to the respiratory demand of the berry in Chardonnay. Seed fresh weight peaks at the beginning of sugar accumulation and skin coloration, with this stage termed veraison (Ristic and Iland, 2005), and was reached ~63 DAA for Chardonnay here. Seed respiration at this stage was 5-fold higher than whole berry respiration on a per gram fresh weight basis. Berry respiration was reduced by about a third at 122 DAA compared with 63 DAA (Fig. 5A); however, seed respiration decreased by 40-fold (Fig. 5B). Berry mass nearly doubled from 7.2 ± 0.5 g at 63 DAA to 13.9 ± 1.4 g at 122 DAA; thus, on a per berry basis, respiration rate increased by ~18% from 63 DAA to 122 DAA (Fig. 5C). The contribution from the total number of seeds in the berry accounted for more than half of the respiratory demand in berries at veraison. This dropped to an insignificant proportion at 122 DAA (Fig. 5C).

Differences in resistance to diffusion into the berry may influence the [O_2] profiles. The pedicel lenticels may offer a pathway for O_2 entry that could account for the higher concentration towards the central axis of the berry. There were obvious differences in lenticel morphology between Chardonnay (Fig. 6A) and Shiraz berries (Fig. 6B). Individual lenticels on Chardonnay pedicels were larger, and also had a 10-fold larger total surface area as a proportion of pedicel surface area compared with that of Shiraz berries (Fig. 6C).

To determine whether lenticels on the pedicel could be sites for berry gas exchange, respiration was measured on the same batches of berries with or without pedicels covered with silicone grease to impede gas exchange. This was examined at 20 °C and 40 °C as respiratory demand for O_2 increases with temperature (Hertog *et al.*, 1998). Figure 7A shows that covering the berry pedicel (and lenticels) with silicone grease decreased berry respiration at 40 °C for both Shiraz and Chardonnay berries, but had no effect on respiration at 20 °C. The temperature dependence of respiration was examined in more detail for Chardonnay and Shiraz, with both yielding similar activation energies and Q_{10} (Supplementary Figs S1, S2 at *JXB* online) that did not differ between berries sampled on the two days for each cultivar. The decreased apparent respiration of berries with the covered pedicel was not due to the elimination of pedicel respiration, because the pedicel respiration rate at 40 °C was a small fraction of the total berry respiration (Fig. 7B) and did not account for the decrease observed when pedicels were covered (Fig. 7A), where the decrease in respiration of pedicel-covered Shiraz and Chardonnay at 40 °C was 839.7 ± 101.8 nmol h^{-1} and 1233.9 ± 229.4 nmol h^{-1} per berry.

A rapid decrease in [O_2] was observed at ~2 mm away from the pedicel and close to the centre axis in the Ruby

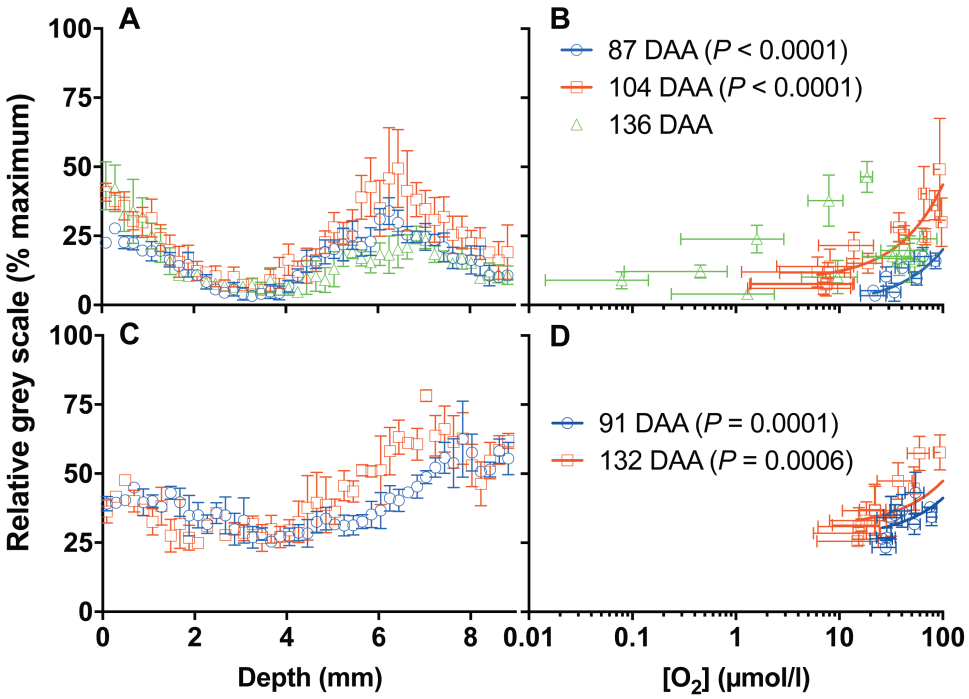

Fig. 3. Correlation between living tissue fluorescence signal and [O_2] profiles. Fluorescence signal [relative grey scale (% maximum)] from FDA stain (high value=higher living tissue) across the radius at the equator of Chardonnay (A) and Ruby Seedless (C). Correlation (Deming regression) between fluorescence signal intensity and [O_2] at corresponding depths (log scale) in Chardonnay on 87 and 104 DAA (B) and Ruby Seedless on 91 and 132 DAA (D) ([O_2] profiles shown in Fig. 1). Data are means ±SE, n=3. (This figure is available in colour at *JXB* online.)

Downloaded from https://academic.oup.com/jxb/article-abstract/69/8/2071/4837303
by University of Adelaide user
on 16 August 2018

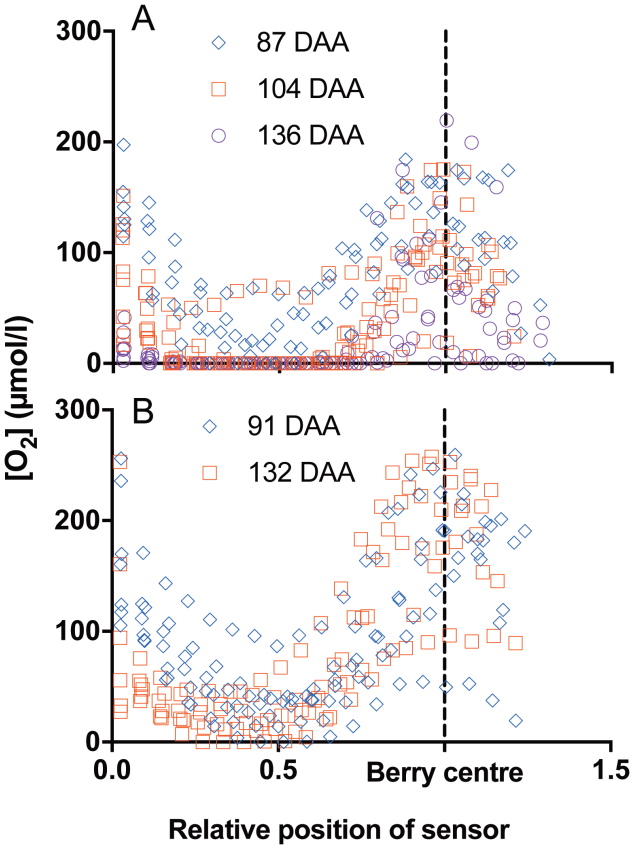

Fig. 4. Individual berry [O_2] profiles normalized to the berry radii. (A) [O_2] profiles of Chardonnay berries sampled at 87, 104, and 136 DAA in the 2015–2016 season (mean data shown in Fig. 2). (B) [O_2] profiles of individual Ruby Seedless berries sampled at 91 and 132 DAA in the 2016–2017 season. (This figure is available in colour at *JXB* online.)

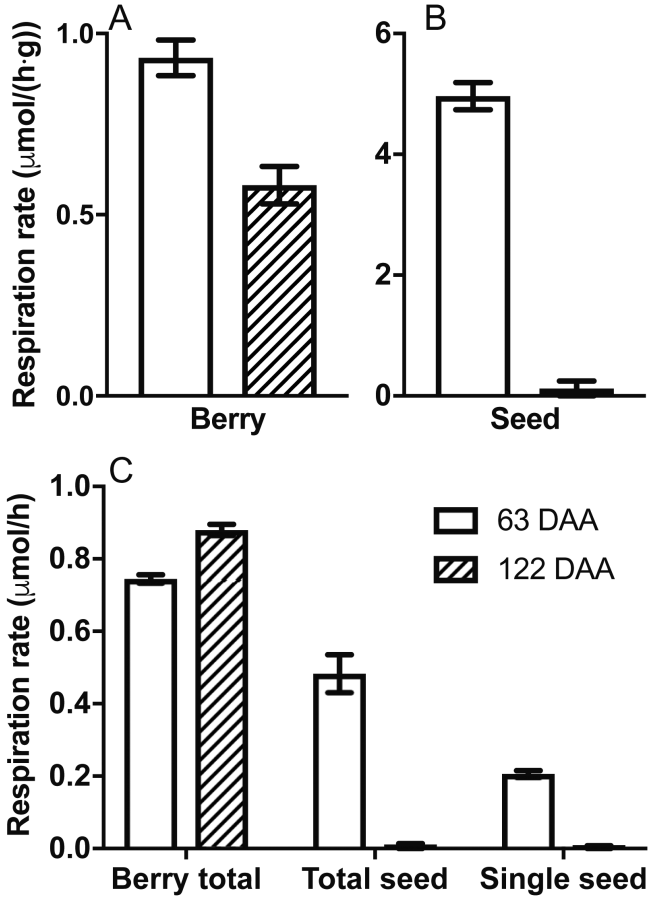

Fig. 5. Chardonnay berry and seed respiration (25 °C) at 63 and 122 DAA in the 2015–2016 season. Respiration on a per gram fresh weight basis for berries (A) and seeds (B). (C) Comparison of respiration rates on a per berry basis (including seeds), total seed basis, and single seed basis. Data are means ±SE, n=3. All rates are different between 63 and 122 DAA (t-test, P<0.05).

Seedless berries, when an N_2 stream was activated over the pedicel (Fig. 8).

An experiment was subsequently conducted using growth chamber-grown Chardonnay vines to test whether covering the pedicel lenticels of berries attached to the vine would affect internal [O_2] profiles. Three days after covering the berry pedicel with silicone grease, a reduction in [O_2] at the central vascular region occurred and remained near 0 μmol l^{-1} over the subsequent 15 d (Fig. 9A). For control berries, a maximum of [O_2] was evident at the central axis across all days of measurement. The concentration of TSS increased with time during the course of this experiment, and was higher for lenticel-covered berries (Fig. 9B). Sugar/berry was not affected by covering the lenticels (Fig. 9C). Ethanol concentration of berries was measured at 12 d and 20 d after covering the pedicel lenticels. These berries, showed higher ethanol content compared with control berries (Fig. 9D), consistent with more fermentation within the hypoxic berries. CD was significantly increased by limiting oxygen diffusion after 10 d of covering the lenticels (Fig. 9E), and this was also evident from examination of transects across the berry (Fig. 9F).

Air spaces within the grape berry shown by micro-CT

Using micro-CT, the internal air spaces of Chardonnay berries at two time points during ripening, where air spaces within the berry were greater in total volume than 500 voxels (1.5×10^{-3} mm^3), are shown in Fig. 10. Colour rendering highlighted air space within the berries for both post-veraison (98 DAA, Fig. 10A) and post-harvest (154 DAA, Fig. 10B) berries. Air spaces were connected to the pedicel in the post-veraison berry, but not obviously in the post-harvest berry. It was evident that there were larger air spaces within the locule. Porosity, pores, and channels, between the berry proximal region and seed(s) hilum, did not differ between berries sampled on the two days (Supplementary Fig. S3).

Discussion

The mesocarp of seeded wine grape berries typically shows a type of programmed CD associated with dehydration and flavour development late in ripening (Tilbrook and Tyerman, 2008; Fuentes *et al.*, 2010; Bonada *et al.*, 2013*b*). Here we show a close similarity between the pattern of CD across the berry mesocarp and [O_2] profiles where the central regions of the mesocarp had both the highest CD and the lowest [O_2]. In both Shiraz and Chardonnay, the oxygen deficit in the centre of the mesocarp increased as ripening and CD progressed,

Downloaded from https://academic.oup.com/jxb/article-abstract/69/8/2071/4837303
by University of Adelaide user
on 16 August 2018

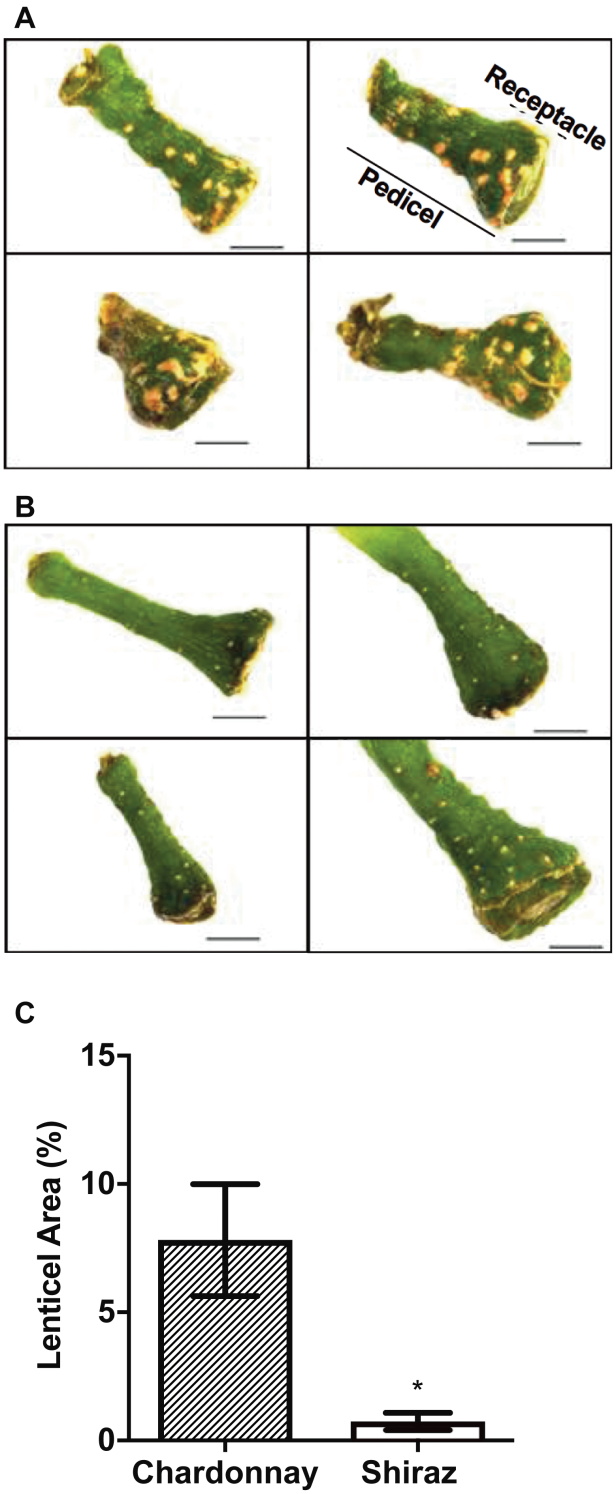

Fig. 6. Differences in lenticel morphology and relative lenticel area between Chardonnay (A) and Shiraz (B) berry pedicels. (C) Lenticel area relative to pedicel surface area of Chardonnay and Shiraz berries (chamber grown, 2015) estimated using ImageJ. Scale bars in (A) and (B)=1 mm. Data in (C) are means ±SE, n=5, *Significantly different (t-test, P<0.05). (This figure is available in colour at *JXB* online.)

essentially becoming anoxic after ~100 d from anthesis under our experimental conditions. This contrasted with the seedless, table grape cultivar where the [O_2] remained above ~15 μmol l^{-1} (1.1 kPa) in the mid region of the mesocarp, still considered to be hypoxic (Saglio *et al.*, 1988), where CD was less apparent. In our experimental system, however, only three cultivars were tested and there is a confounded effect between cultivar types (wine versus table) with different water and sugar dynamics (Sadras *et al.*, 2008) and between seeded and seedless types. Separating these effects would require the comparison of seeded and seedless isogenic lines. Nonetheless, the strong correlation between CD and [O_2] profiles, the role of lenticels, seed respiration, ethanol fermentation, and CT images all converge to support our working hypothesis that hypoxia in the mesocarp contributes to CD in the grape berry.

The minimum [O_2] we measured in the pericarp for both Chardonnay and Shiraz berries (close to zero) may be at or below the K_m for cytochrome *c* oxidase (0.14 μM) (Millar *et al.*, 1994), and very probably resulted in restricted oxidative phosphorylation and a shift to fermentation as evidenced by the detection of ethanol in Chardonnay berries; testing other cultivars for ethanol production would be of interest. All aerobic organisms require O_2 for efficient ATP production through oxidative phosphorylation. Lower ATP production occurs under hypoxia when cells shift from oxidative phosphorylation to fermentation (Ricard *et al.*, 1994; Drew, 1997; Geigenberger, 2003). The depletion of ATP has profound consequences on cell physiology, including a change in energy consumption and cellular metabolism (Drew, 1997; Bailey-Serres and Chang, 2005). Loss of membrane integrity responsible for browning disorder in pears is also linked to internal hypoxia and low ATP levels (Saquet *et al.*, 2003; Franck *et al.*, 2007).

Survival of grape berry mitochondria after imposed anaerobiosis (based on succinate oxidation rates) is cultivar dependent, with survival ranging from 1 d to 10 d (Romieu *et al.*, 1992). This work was based on the process of carbonic maceration, a wine-making procedure where whole berries ferment in an anaerobic atmosphere prior to crushing. Ethanol alters the respiratory quotient of grape mitochondria and uncouples oxidative phosphorylation (Romieu *et al.*, 1992). These effects occurred at >1% (volume) ethanol and well above the concentrations we measured in Chardonnay berries (0.015%); however, it is possible that there are locally high concentrations of ethanol within the berry in our case. In a later study, ADH activity and ADH RNA were found to be already high in field-grown Chardonnay berries before anaerobiosis treatment, suggesting that a hypoxic situation already existed in the grapes as a result of some stressful conditions in the field (Tesnière *et al.*, 1993). Our results show that this may be the norm for certain regions within the berry mesocarp and is likely to be exacerbated by high temperature (see below).

The internal [O_2] of fruit depends on the respiratory demand, and the O_2 diffusion properties of the skin and internal tissues. These can show genotypic differences as is the case for apple fruit (Ho *et al.*, 2010). In pear fruit, differences in porosity of the cortex, the connectivity of intercellular spaces, and cell distribution may account for variation between cultivars (Ho *et al.*, 2009). For pear it was possible to reconcile the observed variation in gas diffusion with the irregular microstructure of the tissue using a microscale model of gas diffusion. This also appears to be the case for different cultivars of apple as assessed by micro-CT (Mendoza *et al.*, 2007). For grape berries, the

Downloaded from https://academic.oup.com/jxb/article-abstract/69/8/2071/4837303
by University of Adelaide user
on 16 August 2018

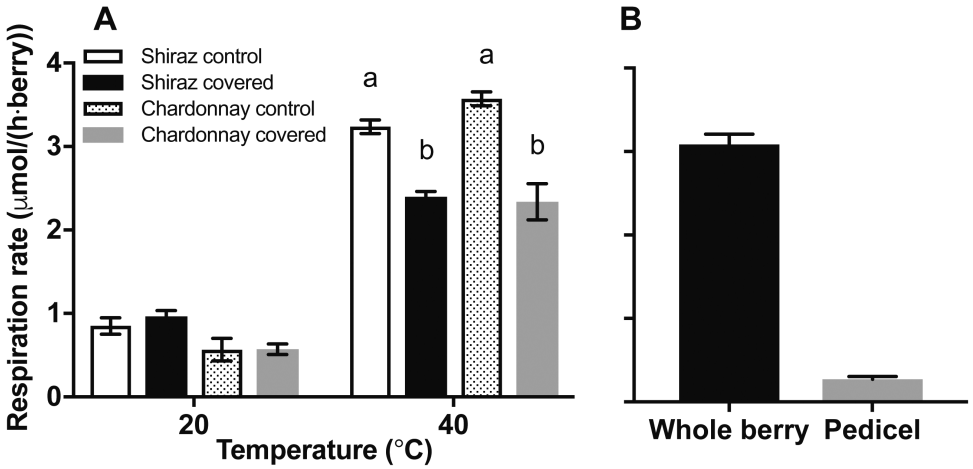

Fig. 7. Role of the pedicel in oxygen diffusion as a function of temperature. (A) Respiration of Chardonnay (86 DAA) and Shiraz (77 DAA) berries (per berry basis) at 20 °C and 40 °C with pedicels attached (the 2016–2017 season). Silicone grease covered the lenticels on the pedicel (covered berries). At 20 °C, no significant difference in apparent berry respiration was found between control and pedicel-covered berries for both cultivars. Different lower case letters indicate significant differences between treatments at 40 °C within each cultivar (two-way ANOVA, $P<0.0001$). Shiraz and Chardonnay showed a decrease of 839.7 ± 101.8 nmol h^{-1} and 1377.3 ± 161.3 nmol h^{-1} per berry in respiration at 40 °C (26% and 39% decrease), respectively. (B) Respiration rate of whole berry including attached pedicel and respiration of separated pedicels for Chardonnay at 40 °C. The pedicel accounted for 9% of the whole berry respiration rate. Data are means ±SE, n=3.

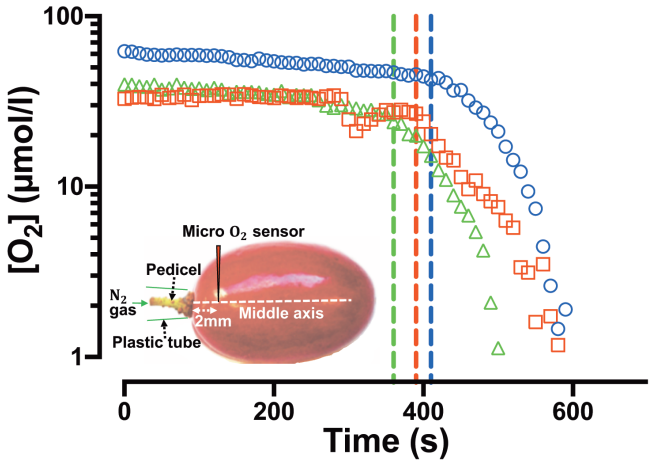

Fig. 8. The role of the pedicel in gas diffusion into Ruby Seedless grapes (132 DAA in the 2016–2017 season). $[O_2]$ of three individual berries as a function of time with the sensor inserted approximately at the central axis of Ruby Seedless ~2 mm from the pedicel. Dashed lines indicate the start of external N_2 gas delivery over the pedicel. Different symbols indicate different berries. Inset: experimental set-up for applying N_2 gas over the berry pedicel while measuring $[O_2]$. (This figure is available in colour at *JXB* online.)

$[O_2]$ profiles in our study would suggest a very low O_2 diffusivity for the skin since a steep gradient occurred across the skin. Apple skin also showed a very low O_2 diffusivity and likewise a steep concentration gradient across the skin (Ho *et al.*, 2010). Since sub-skin $[O_2]$ of grape berries declined dramatically during ripening for all three grape cultivars, it would suggest a decline in O_2 diffusivity during ripening that may result from the same epidermal and cuticle structural changes that cause a decline in berry transpiration (Rogiers *et al.*, 2004).

Changing properties of the skin, berry porosity and lenticels in the pedicel may all contribute to the reduced internal $[O_2]$ in grape berries during ripening. Fruit parenchyma can be regarded as a porous medium with air spaces distributed in between the elliptically tessellated cells (Gray *et al.*, 1999; Mebatsion *et al.*, 2006; Herremans *et al.*, 2015). A maximum $[O_2]$ at the central axis region of both seeded and seedless berries throughout berry development indicates a channel connecting the source of O_2 intake and the central vascular bundles. Using different approaches, including blockage of pedicel lenticels with silicone grease or applying of N_2 over pedicels, our experiments demonstrated that the pedicel lenticels are a major pathway for O_2 diffusion into the grape berry. This corresponds to the predominant air canals observed in micro-CT from the receptacle into the central axis of the berry. Micro-CT to study air space distributions in fruit can reveal important properties that affect gas diffusion (Mendoza *et al.*, 2010; Herremans *et al.*, 2015) as well as internal disorders (Lammertyn *et al.*, 2003). In our work, the visualization of air space connecting the pedicel with the locular cavity around seeds provides the structural link to the measured peaks in $[O_2]$ around the central vascular region in the berries. This also confirmed the potential O_2 uptake pathway through the pedicel lenticels, and distribution through the vascular networks. The relatively higher $[O_2]$ around both central and peripheral vascular bundles may be important for maintaining phloem unloading in the berry, and it is interesting to note that even with severe CD in berries, the vascular bundles generally remain vital (Fuentes *et al.*, 2010). Despite this, we observed higher sugar concentrations in hypoxic berries that had their lenticels covered while still on the vine. This anomaly may be accounted for by decreased water influx because of hypoxia, thereby causing an increase in sugar concentration. Hypoxia is associated with reduced plasma membrane water permeability (Zhang and Tyerman, 1991) caused by closing of water channels of the plasma membrane intrinsic protein (PIP) family (Tournaire-Roux *et al.*, 2003). This is due to sensitivity to lowered cytosolic pH under hypoxia. A PIP aquaporin gene (*VvPIP2;1*) that is highly expressed in the ripening berry (Choat *et al.*, 2009) would be predicted to have reduced water

Downloaded from https://academic.oup.com/jxb/article-abstract/69/8/2071/4837303
by University of Adelaide user
on 16 August 2018

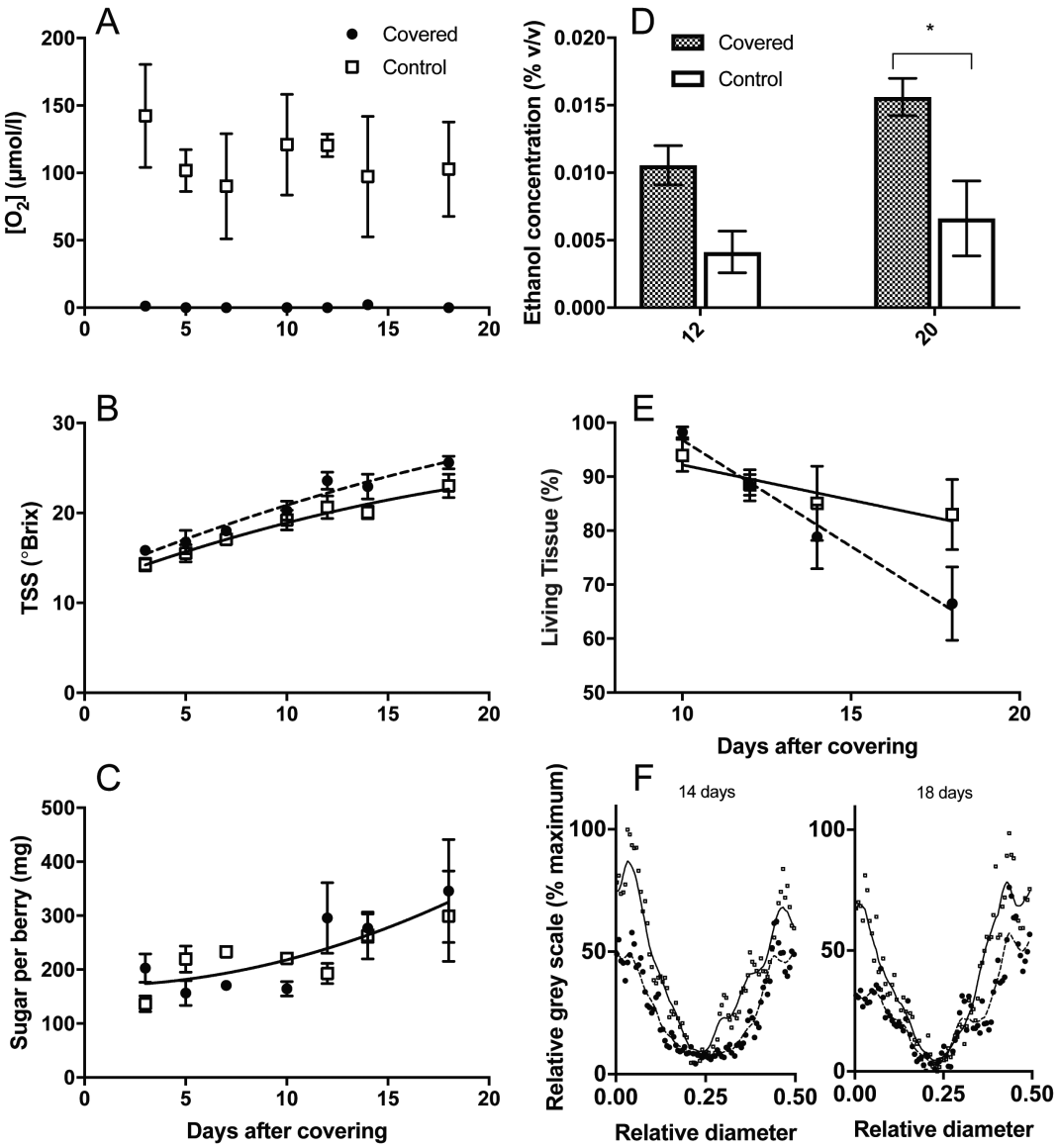

Fig. 9. The effect of covering berry pedicels with silicone grease on intact Chardonnay clusters during ripening (chamber grown 2017, open squares=control, filled circles =covered). (A) $[O_2]$ at the approximate centre axis of berries as a function of time after covering pedicels. Two-way ANOVA showed that covering pedicels reduced $[O_2]$ ($P<0.0001$). (B) Total soluble solids (TSS) concentration of berries as a function of time after covering pedicels. Pedicel-covered berries showed significantly higher TSS during the course of the experiment compared with control berries (two-way ANOVA $P=0.003$; fits are second-order polynomials, solid line=control, dashed line=covered). (C) Sugar per berry as a function of time after covering pedicels. No significant difference was found between treatments in sugar/berry (combined fit is a second-order polynomial, solid line). (D) Ethanol concentration of berries after 12 d and 20 d with (filled) and without (open) silicone grease covering the pedicels. Two-way ANOVA (Tukey's multiple comparisons test) showed a significant difference at 20 d after covering ($P=0.036$). (E) Percentage living tissue as a function of time. The slope of the fitted line for covered berries (dashed line) is non-zero ($P=0.008$) and different from the slope of the fitted line (solid line) for uncovered berries ($P=0.006$). (F) Fluorescence signal (FDA stain, relative to maximum, high value=higher living tissue) across the radius at the equator normalized for variation in berry diameter at 14 d and 18 d after covering. Locally weighted scatterplot smoothing fits (LOWESS) are shown for each. Covered (dashed line) versus control (solid line) are significantly different at both times (two-way ANOVA, $P<0.001$). Data are means ±SE, $n=3$, except (F) where SEs are not shown.

permeation under hypoxia (Tournaire-Roux *et al.*, 2003), perhaps accounting for the decrease in whole berry hydraulic conductance that is consistently observed for Chardonnay and Shiraz (Tilbrook and Tyerman, 2009; Scharwies and Tyerman, 2017).

Lenticels are multicellular structures produced from phellogen that replace stomata after secondary growth (Lendzian, 2006). The impact of lenticels on gas and water permeance compared with periderm of stems has been measured for some species. For *Betula pendula*, the presence of lenticels substantially increased the water permeability of the periderm by between 26- and 53-fold (Schönherr and Ziegler, 1980). Lenticels on the berry pedicel are a preferential site for water uptake for submerged detached berries (Becker *et al.*, 2012). Water vapour and O_2 permeance of tree phellem with and without lenticels showed that lenticels increased O_2 permeance much more than that for water, >1000-fold for one species, yet the permeance for water vapour was higher than that for O_2 (Groh *et al.*, 2002). Interestingly, Schönherr and Ziegler (1980) showed that as the water vapour activity declined (increased vapour

Downloaded from https://academic.oup.com/jxb/article-abstract/69/8/2071/4837303
by University of Adelaide user
on 16 August 2018

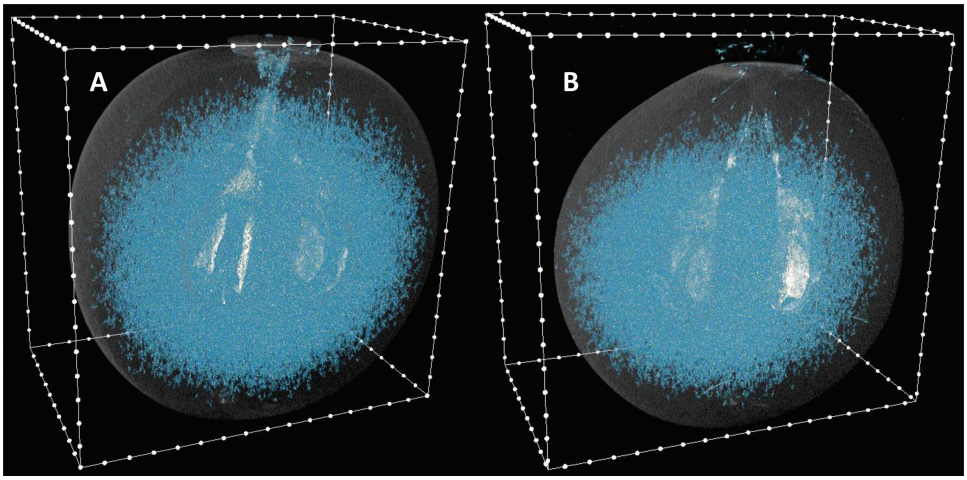

Fig. 10. Air spaces in Chardonnay berries as determined by X-ray micro-CT. (A) At 98 DAA (19.3 °Brix) and (B) at 154 DAA (24.5 °Brix) in the 2015–2016 season. Images have been manipulated to indicate the berry outline. Minimum voxel cut-off was 500. White dots on the box outline are at 1 mm intervals.

pressure deficit), water permeability was strongly reduced. If declining water vapour activity also reduced O_2 permeability in grape berry lenticels, this could restrict O_2 diffusion under the very conditions where respiratory demand is increased, namely under water stress and with high temperature and vapour pressure deficit.

The decrease in $[O_2]$ at the approximate central axis in the seeded Chardonnay berry during development suggests there could be either an increase in respiratory demand, a decrease in the intake of O_2 via the pedicel lenticels, or decreased porosity through the central proximal axis. Ruby Seedless berries, on the other hand, did not show this reduction. This indicates that there could be structural differences in lenticels between the seeded wine grape cultivar and the seedless table grape, or that the seeds themselves become a significant O_2 sink (unlikely based on the arguments presented below). The lower lenticel surface area in Shiraz could be indicative of a greater restriction to O_2 diffusion compared with Chardonnay. Shiraz is well known for its earlier and more rapid increase in CD under warm conditions (Fuentes *et al.*, 2010; Bonada *et al.*, 2013*a*). Unfortunately, it was not possible for us to probe for $[O_2]$ in the central region of the Shiraz berry to compare with Chardonnay due to not being able to visualize seed position relative to the sensor in Shiraz berries. The role of the pedicel lenticels in allowing grape berries to 'breathe' and their variation between cultivars seems to have been overlooked and appears to be unique among fruit. Cluster compactness and pedicel length could also affect the gas diffusion via this passage, ultimately resulting in differences in berry internal oxygen availability throughout ripening.

Another possible explanation for the difference in oxygen profiles between the seeded and seedless cultivars is that seeds are a significant O_2 sink late in ripening. Oxygen supply to seeds is essential for seed growth, and deposition of protein and oil (Borisjuk and Rolletschek, 2009). On the other hand, low $[O_2]$ within seeds favours low levels of ROS, thus preventing cellular damage (Simontacchi *et al.*, 1995). The seeded wine grape cultivars Riesling and Bastardo increased O_2 uptake from <0.45 μmol h^{-1} per berry to ~3 μmol h^{-1} per berry during early ripening, contrasting with seedless Sultana where the maximum O_2 uptake was 1.5 μmol h^{-1} per berry (Harris *et al.*, 1971). We observed that total seed respiration was more than half of whole berry respiration at around the beginning of ripening. This high O_2 demand from seeds, prior to the lignification of the outer layer (Cadot *et al.*, 2006), may create a significant O_2 demand within the berry that could lower $[O_2]$ in the locule, and potentially lowering the $[O_2]$ in the mesocarp. However, seed respiration in Chardonnay dramatically declined later in ripening, accounting for the decrease in berry respiration on a per gram basis. During late ripening, $[O_2]$ in the mesocarp of the seeded cultivar dropped to almost zero. Therefore, it is unlikely that the lower $[O_2]$ in the mesocarp was caused by a respiratory demand from seeds directly.

Increased temperature advances the onset and increases the rate of CD in Chardonnay and Shiraz berries (Bonada *et al.*, 2013*a*). Using a modelling approach for pear fruit, it was shown that increasing temperature should strongly increase the respiration rate but should not affect the gas diffusion properties, resulting in predicted very low core $[O_2]$ (Ho *et al.*, 2009). Our direct measures of berry mesocarp $[O_2]$ profiles concur with this prediction. We also observed typical Q_{10} and activation energy for respiration of 2.47 and 2.27 for whole berry respiration rates between 10 °C and 40 °C for Chardonnay and Shiraz berries, respectively, and it was only at 40 °C that blocking the pedicel lenticels reduced respiration. The activation energies were similar to those reported by Hertog *et al.* (1998) for apple (52 875 J mol^{-1}), chicory (67 139 J mol^{-1}), and tomato (67 338 J mol^{-1}). Unlike pear fruit, wine grape berries ripen on the plant and can become considerably hotter than the surrounding air (Smart and Sinclair, 1976; Tarara *et al.*, 2008; Caravia *et al.*, 2016). Transient high temperatures would create a large respiratory demand and low $[O_2]$ in the centre of the mesocarp as we observed. However, subsequent cooling during the night or during milder weather will reduce the respiratory demand and increase internal $[O_2]$ if the diffusivity for O_2 remains the same. This could then result in production of damaging ROS that may cause unrecoverable cell damage (Pfister-Sieber and Braendle, 1994; Rawyler *et al.*, 2002).

Downloaded from https://academic.oup.com/jxb/article-abstract/69/8/2071/4837303
by University of Adelaide user
on 16 August 2018

Conclusion

Grape internal [O_2] declines during fruit development and is correlated with the profile of mesocarp cell death. Lenticels on the pedicel provide a pathway for O_2 diffusion into the berry and, when covered to restrict O_2 diffusion into the berry, cause a large reduction in [O_2] in the centre of the berry, an increase in ethanol concentration, and cell death. Differences in internal O_2 availability of berries between cultivars could be associated with seed development and differences in lenticel surface area. The data presented here provide the basis for further research into the role of berry gas exchange in berry quality and cultivar selection for adapting viticulture to a warming climate.

Supplementary data

Supplementary data are available at *JXB* online.

Fig. S1. Temperature dependence of berry respiration rate.

Fig. S2. Respiratory Q_{10} of Chardonnay and Shiraz berries in response to short-term measurement temperature at two maturity stages.

Fig. S3. Micro-CT analysis of air spaces in Chardonnay berries at two development stages.

Acknowledgements

We thank Wendy Sullivan for expert technical assistance, and Adelaide Microscopy for their facilities and technical support. This research was conducted by the Australian Research Council (ARC) Training Centre for Innovative Wine Production (www.adelaide.edu.au/tc-iwp/), which is funded as a part of the ARC's Industrial Transformation Research Program (Project No. IC130100005) with support from Wine Australia and industry partners.

References

Alexander LV, Arblaster JM. 2009. Assessing trends in observed and modelled climate extremes over Australia in relation to future projections. International Journal of Climatology **29,** 417–435.

Baby T, Hocking B, Tyerman SD, Gilliham M, Collins C. 2014. Modified method for producing grapevine plants in controlled environments. American Journal of Enology and Viticulture **65,** 261–266.

Bailey-Serres J, Chang R. 2005. Sensing and signalling in response to oxygen deprivation in plants and other organisms. Annals of Botany **96,** 507–518.

Becker T, Grimm E, Knoche M. 2012. Substantial water uptake into detached grape berries occurs through the stem surface. Australian Journal of Grape and Wine Research **18,** 109–114.

Blokhina OB, Chirkova TV, Fagerstedt KV. 2001. Anoxic stress leads to hydrogen peroxide formation in plant cells. Journal of Experimental Botany **52,** 1179–1190.

Blokhina O, Virolainen E, Fagerstedt KV. 2003. Antioxidants, oxidative damage and oxygen deprivation stress: a review. Annals of Botany **91,** 179–194.

Bonada M, Sadras VO. 2015. Review: critical appraisal of methods to investigate the effect of temperature on grapevine berry composition. Australian Journal of Grape and Wine Research **21,** 1–17.

Bonada M, Sadras VO, Fuentes S. 2013*a*. Effect of elevated temperature on the onset and rate of mesocarp cell death in berries of Shiraz and Chardonnay and its relationship with berry shrivel. Australian Journal of Grape and Wine Research **19,** 87–94.

Bonada M, Sadras V, Moran M, Fuentes S. 2013*b*. Elevated temperature and water stress accelerate mesocarp cell death and shrivelling, and decouple sensory traits in Shiraz berries. Irrigation Science **31,** 1317–1331.

Bondada B, Keller M. 2012. Not all shrivels are created equal—morpho-anatomical and compositional characteristics differ among different shrivel types that develop during ripening of grape (*Vitis vinifera* L.) berries. American Journal of Plant Sciences **3,** 879–898.

Borisjuk L, Rolletschek H. 2009. The oxygen status of the developing seed. New Phytologist **182,** 17–30.

Bottcher C, Harvey KE, Boss PK, Davies C. 2013. Ripening of grape berries can be advanced or delayed by reagents that either reduce or increase ethylene levels. Functional Plant Biology **40,** 566–581.

Cadot Y, Miñana-Castelló MT, Chevalier M. 2006. Anatomical, histological, and histochemical changes in grape seeds from *Vitis vinifera* L. cv Cabernet franc during fruit development. Journal of Agricultural and Food Chemistry **54,** 9206–9215.

Caravia L, Collins C, Petrie PR, Tyerman SD. 2016. Application of shade treatments during Shiraz berry ripening to reduce the impact of high temperature. Australian Journal of Grape and Wine Research **22,** 422–437.

Caravia L, Collins C, Tyerman SD. 2015. Electrical impedance of Shiraz berries correlates with decreasing cell vitality during ripening. Australian Journal of Grape and Wine Research **21,** 430–438.

Choat B, Gambetta GA, Shackel KA, Matthews MA. 2009. Vascular function in grape berries across development and its relevance to apparent hydraulic isolation. Plant Physiology **151,** 1677–1687.

Coombe BG. 1973. The regulation of set and development of the grape berry. Acta Horticulturae **34,** 261–274.

Coombe BG. 1995. Growth stages of the grapevine: adoption of a system for identifying grapevine growth stages. Australian Journal of Grape and Wine Research **1,** 104–110.

Drew MC. 1997. Oxygen deficiency and root metabolism: injury and acclimation under hypoxia and anoxia. Annual Review of Plant Physiology and Plant Molecular Biology **48,** 223–250.

Du Toit PG. 2005. The effect of partial rootzone drying on the partitioning of dry matter, carbon, nitrogen and inorganic ions of grapevines. PhD thesis, The University of Adelaide, Australia.

Famiani F, Farinelli D, Palliotti A, Moscatello S, Battistelli A, Walker RP. 2014. Is stored malate the quantitatively most important substrate utilised by respiration and ethanolic fermentation in grape berry pericarp during ripening? Plant Physiology and Biochemistry **76,** 52–57.

Franck C, Lammertyn J, Ho QT, Verboven P, Verlinden B, Nicolaï BM. 2007. Browning disorders in pear fruit. Postharvest Biology and Technology **43,** 1–13.

Fuentes S, Sullivan W, Tilbrook J, Tyerman S. 2010. A novel analysis of grapevine berry tissue demonstrates a variety-dependent correlation between tissue vitality and berry shrivel. Australian Journal of Grape and Wine Research **16,** 327–336.

Fukao T, Bailey-Serres J. 2004. Plant responses to hypoxia—is survival a balancing act? Trends in Plant Science **9,** 449–456.

Geigenberger P. 2003. Response of plant metabolism to too little oxygen. Current Opinion in Plant Biology **6,** 247–256.

Gray JD, Kolesik P, Høj PB, Coombe BG. 1999. Technical advance: confocal measurement of the three-dimensional size and shape of plant parenchyma cells in a developing fruit tissue. The Plant Journal **19,** 229–236.

Groh B, Hübner C, Lendzian KJ. 2002. Water and oxygen permeance of phellems isolated from trees: the role of waxes and lenticels. Planta **215,** 794–801.

Hardie WJ, O'Brien TP, Jaudzems VG. 1996. Morphology, anatomy and development of the pericarp after anthesis in grape, *Vitis vinifera* L. Australian Journal of Grape and Wine Research **2,** 97–142.

Harris J, Kriedemann P, Possingham J. 1971. Grape berry respiration: effects of metabolic inhibitors. Vitis **9,** 291–298.

Herremans E, Verboven P, Verlinden BE, Cantre D, Abera M, Wevers M, Nicolaï BM. 2015. Automatic analysis of the 3-D microstructure of fruit parenchyma tissue using X-ray micro-CT explains differences in aeration. BMC Plant Biology **15,** 264.

Hertog MLATM, Peppelenbos HW, Evelo RG, Tijskens LMM. 1998. A dynamic and generic model of gas exchange of respiring produce: the effects of oxygen, carbon dioxide and temperature. Postharvest Biology and Technology **14,** 335–349.

Ho QT, Verboven P, Mebatsion HK, Verlinden BE, Vandewalle S, Nicolaï BM. 2009. Microscale mechanisms of gas exchange in fruit tissue. New Phytologist **182,** 163–174.

Downloaded from https://academic.oup.com/jxb/article-abstract/69/8/2071/4837303
by University of Adelaide user
on 16 August 2018

Ho QT, Verboven P, Verlinden BE, Schenk A, Delele MA, Rolletschek H, Vercammen J, Nicolaï BM. 2010. Genotype effects on internal gas gradients in apple fruit. Journal of Experimental Botany **61,** 2745–2755.

Keller M, Shrestha PM. 2014. Solute accumulation differs in the vacuoles and apoplast of ripening grape berries. Planta **239,** 633–642.

Keller M, Shrestha PM, Hall GE, Bondada BR, Davenport JR. 2016. Arrested sugar accumulation and altered organic acid metabolism in grape berries affected by berry shrivel syndrome. American Journal of Enology and Viticulture **67,** 398–406.

Krasnow M, Matthews M, Shackel K. 2008. Evidence for substantial maintenance of membrane integrity and cell viability in normally developing grape (*Vitis vinifera* L.) berries throughout development. Journal of Experimental Botany **59,** 849–859.

Kriedemann P. 1968. Observations on gas exchange in the developing Sultana berry. Australian Journal of Biological Sciences **21,** 907–916.

Lammertyn J, Dresselaers T, Van Hecke P, Jancsok P, Wevers M, Nicolai BM. 2003. Analysis of the time course of core breakdown in 'Conference' pears by means of MRI and X-ray CT. Postharvest Biology and Technology **29,** 19–28.

Lee Y, Rubio MC, Alassimone J, Geldner N. 2013. A mechanism for localized lignin deposition in the endodermis. Cell **153,** 402–412.

Lendzian KJ. 2006. Survival strategies of plants during secondary growth: barrier properties of phellems and lenticels towards water, oxygen, and carbon dioxide. Journal of Experimental Botany **57,** 2535–2546.

Mebatsion H, Verboven P, Ho Q, Verlinden B, Mendoza F, Nguyen T, Nicolaï B. 2006. Modeling fruit microstructure using an ellipse tessellation algorithm. Computer Modeling in Engineering & Sciences **14,** 1–14.

Mendoza F, Verboven P, Ho QT, Kerckhofs G, Wevers M, Nicolai B. 2010. Multifractal properties of pore-size distribution in apple tissue using X-ray imaging. Journal of Food Engineering **99,** 206–215.

Mendoza F, Verboven P, Mebatsion HK, Kerckhofs G, Wevers M, Nicolaï B. 2007. Three-dimensional pore space quantification of apple tissue using X-ray computed microtomography. Planta **226,** 559–570.

Millar A, Bergersen F, Day D. 1994. Oxygen affinity of terminal oxidases in soybean mitochondria. Plant Physiology and Biochemistry **32,** 847–852.

Ollat N, Gaudillère J. 1997. Carbon balance in developing grapevine berries. Acta Horticulturae **526,** 345–350.

Palliotti A, Cartechini A. 2001. Developmental changes in gas exchange activity in flowers, berries, and tendrils of field-grown Cabernet Sauvignon. American Journal of Enology and Viticulture **52,** 317–323.

Perkins SE, Alexander LV, Nairn JR. 2012. Increasing frequency, intensity and duration of observed global heatwaves and warm spells. Geophysical Research Letters **39,** 20714.

Pfister-Sieber M, Braendle R. 1994. Aspects of plant behaviour under anoxia and post-anoxia. Proceedings of the Royal Society of Edinburgh, Section B: Biological Sciences **102,** 313–324.

Pilati S, Brazzale D, Guella G, Milli A, Ruberti C, Biasioli F, Zottini M, Moser C. 2014. The onset of grapevine berry ripening is characterized by ROS accumulation and lipoxygenase-mediated membrane peroxidation in the skin. BMC Plant Biology **14,** 87.

Rawyler A, Arpagaus S, Braendle R. 2002. Impact of oxygen stress and energy availability on membrane stability of plant cells. Annals of Botany **90,** 499–507.

Ricard B, Couée I, Raymond P, Saglio PH, Saint-Ges V, Pradet A. 1994. Plant metabolism under hypoxia and anoxia. Plant Physiology and Biochemistry **32,** 1–10.

Ristic R, Iland PG. 2005. Relationships between seed and berry development of *Vitis vinifera* L. cv Shiraz: developmental changes in seed morphology and phenolic composition. Australian Journal of Grape and Wine Research **11,** 43–58.

Rogiers SY, Hatfield JM, Jaudzems VG, White RG, Keller M. 2004. Grape berry cv. Shiraz epicuticular wax and transpiration during ripening and preharvest weight loss. American Journal of Enology and Viticulture **55,** 121–127.

Romieu C, Tesniere C, Than-Ham L, Flanzy C, Robin J-P. 1992. An examination of the importance of anaerobiosis and ethanol in causing injury to grape mitochondria. American Journal of Enology and Viticulture **43,** 129–133.

Sadras V, Collins M, Soar C. 2008. Modelling variety-dependent dynamics of soluble solids and water in berries of *Vitis vinifera*. Australian Journal of Grape and Wine Research **14,** 250–259.

Sadras VO, McCarthy MG. 2007. Quantifying the dynamics of sugar concentration in berries of *Vitis vinifera* cv. Shiraz: a novel approach based on allometric analysis. Australian Journal of Grape and Wine Research **13,** 66–71.

Saglio PH, Drew MC, Pradet A. 1988. Metabolic acclimation to anoxia induced by low (2-4 kPa partial pressure) oxygen pretreatment (hypoxia) in root tips of *Zea mays*. Plant Physiology **86,** 61–66.

Saquet AA, Streif J, Bangerth F. 2003. Energy metabolism and membrane lipid alterations in relation to brown heart development in 'Conference' pears during delayed controlled atmosphere storage. Postharvest Biology and Technology **30,** 123–132.

Sasidharan R, Bailey-Serres J, Ashikari M, *et al*. 2017. Community recommendations on terminology and procedures used in flooding and low oxygen stress research. New Phytologist **214,** 1403–1407.

Scharwies JD, Tyerman SD. 2017. Comparison of isohydric and anisohydric *Vitis vinifera* L. cultivars reveals a fine balance between hydraulic resistances, driving forces and transpiration in ripening berries. Functional Plant Biology **44,** 324–338.

Schneider CA, Rasband WS, Eliceiri KW. 2012. NIH image to ImageJ: 25 years of image analysis. Nature Methods **9,** 671–675.

Schönherr J, Ziegler H. 1980. Water permeability of Betula periderm. Planta **147,** 345–354.

Simontacchi M, Caro A, Puntarulo S. 1995. Oxygen-dependent increase of antioxidants in soybean embryonic axes. International Journal of Biochemistry and Cell Biology **27,** 1221–1229.

Smart RE, Sinclair TR. 1976. Solar heating of grape berries and other spherical fruits. Agricultural Meteorology **17,** 241–259.

Strike PW. 1991. Measurement and control. Statistical methods in laboratory medicine. Oxford: Butterworth-Heinemann, 254–306.

Šuklje K, Zhang X, Antalick G, Clark AC, Deloire A, Schmidtke LM. 2016. Berry shriveling significantly alters shiraz (*Vitis vinifera* L.) grape and wine chemical composition. Journal of Agricultural and Food Chemistry **64,** 870–880.

Tarara JM, Lee J, Spayd SE, Scagel CF. 2008. Berry temperature and solar radiation alter acylation, proportion, and concentration of anthocyanin in merlot grapes. American Journal of Enology and Viticulture **59,** 235–247.

Terrier N, Romieu C. 2001. Grape berry acidity. In: Roubelakis-Angelakis KA, ed. Molecular biology & biotechnology of the grapevine. Dordrecht: Springer Netherlands, 35–57.

Tesnière CM, Romieu C, Vayda ME. 1993. Changes in the gene expression of grapes in response to hypoxia. American Journal of Enology and Viticulture **44,** 445–451.

Tilbrook J, Tyerman SD. 2008. Cell death in grape berries: varietal differences linked to xylem pressure and berry weight loss. Functional Plant Biology **35,** 173–184.

Tilbrook J, Tyerman SD. 2009. Hydraulic connection of grape berries to the vine: varietal differences in water conductance into and out of berries, and potential for backflow. Functional Plant Biology **36,** 541–550.

Tournaire-Roux C, Sutka M, Javot H, Gout E, Gerbeau P, Luu DT, Bligny R, Maurel C. 2003. Cytosolic pH regulates root water transport during anoxic stress through gating of aquaporins. Nature **425,** 393–397.

Voesenek LA, Colmer TD, Pierik R, Millenaar FF, Peeters AJ. 2006. How plants cope with complete submergence. New Phytologist **170,** 213–226.

Webb LB, Whetton PH, Barlow EWR. 2007. Modelled impact of future climate change on the phenology of winegrapes in Australia. Australian Journal of Grape and Wine Research **13,** 165–175.

Wigginton MJ. 1973. Diffusion of oxygen through lenticels in potato tuber. Potato Research **16,** 85–87.

Zhang W, Tyerman S. 1991. Effect of low O_2 concentration and azide on hydraulic conductivity and osmotic volume of the cortical cells of wheat roots. Functional Plant Biology **18,** 603–613.

Downloaded from https://academic.oup.com/jxb/article-abstract/69/8/2071/4837303
by University of Adelaide user
on 16 August 2018